

Ideal Passivation of Luminescent Porous Silicon by Thermal, Noncatalytic Reaction with Alkenes and Aldehydes[†]

R. Boukherroub,^{*,‡} S. Morin,[‡] D. D. M. Wayner,^{*,‡} F. Bensebaa,[§] G. I. Sproule,^{||} J.-M. Baribeau,^{||} and D. J. Lockwood^{*,||}

Stecie Institute for Molecular Sciences, Institute for Chemical Process and Environmental Technology, and Institute for Microstructural Sciences, National Research Council of Canada, Ottawa, Ontario, Canada K1A 0R6

Received October 2, 2000. Revised Manuscript Received January 27, 2001

This paper describes the chemical modification of high surface area, photoluminescent porous silicon (PSi) by reaction at a moderately elevated temperature (<115 °C) with alkenes (RCH=CH₂) and aldehydes (RCHO) to give organic monolayers covalently bonded to the surface through Si–C and Si–O–C linkages, respectively. The monolayers are characterized using diffuse reflectance infrared Fourier transform (DRIFT), transmission FTIR, Raman, X-ray photoelectron, and Auger spectroscopies. Auger depth profiling results are consistent with homogeneous incorporation of organic molecules on the internal surface of the PSi. The functionalized surfaces demonstrate high chemical stability in boiling aqueous and organic solvents and even in harsher environments such as aqueous HF or KOH. Aging in ambient air for several months has no effect on the PL intensity or energy. Notably, when the surfaces were treated at 100 percent humidity at 70 °C for 6 weeks, only a small increase in the PL intensity was observed. This severe treatment completely transformed H-terminated PSi into a transparent oxide layer. This result is consistent with the formation of organic films with a very low defect density at the interface. Thus, these organic monolayers have unprecedented stability and ideally passivate the PSi.

Introduction

Since the first report on the efficient visible photoluminescence (PL) of porous silicon (PSi) under UV excitation, at room temperature, this material has generated worldwide interest.¹ There has been a vast amount of work devoted to the structural, optical, and electronic aspects of this material to understand the origins of the PL and to develop applications in solid-state electroluminescent devices.² Because of its tunable electroluminescent and photoluminescent properties, applications in silicon-based optoelectronics, which have hitherto been severely constrained by the weak luminescence of indirect band-gap bulk silicon, became feasible. The origin of the quantum-confined PL is assigned to the Si nanocrystallites present in the porous layer. Several models have been proposed to explain the PL contributions from other species on the PSi surface.² Potential applications based on electrical and/or optical measurements for sensing chemical^{3–7} and biochemical^{8–11} species have been demonstrated using PSi.

A freshly prepared PSi surface is covered with a monolayer of hydrogen (Si–H_x). The hydrogen-passivated PSi film is of good electronic quality,^{1,2} but the monolayer of hydrogen formed on its surface does not protect against PL quenching from chemical adsorbates, leading to slow degradation of PL exposure to air¹³ and concomitant degradation of the electronic properties of the material. This limitation restricts the use of PSi in the fabrication of commercial devices. The hydrogen-terminated PSi surface reacts in ambient air to form an oxide submonolayer, which introduces the surface defects responsible for the PL quenching. Many efforts have been made to stabilize the H-terminated surface

(4) Motohashi, A.; Ruike, M.; Kawakami, M.; Aoyagi, H.; Kinoshita, A.; Satou, A. *Jpn. J. Appl. Phys., Part 1* **1996**, *35*, 4523.

(5) Ben-Chorin, M.; Kux, A.; Schechter, I. *Appl. Phys. Lett.* **1994**, *64*, 481.

(6) Schechter, I.; Ben-Chorin, M.; Kux, A. *Anal. Chem.* **1995**, *67*, 3727.

(7) Watanabe, K.; Okada, T.; Choe, I.; Sato, Y. *Sens. Actuators B* **1996**, *33*, 194.

(8) Lin, V. S.-Y.; Moteshareh, K.; Dancil, K.-P. S.; Sailor, M. J.; Ghadiri, M. R. *Science* **1997**, *278*, 840.

(9) Janshoff, A.; Dancil, K.-P. S.; Steinem, C.; Greiner, D. P.; Lin, V. S.-Y.; Gurtner, C.; Moteshareh, K.; Sailor, M. J.; Ghadiri, M. R. *J. Am. Chem. Soc.* **1998**, *120*, 12108.

(10) Dancil, K.-P. S.; Greiner, D. P.; Sailor, M. J. *J. Am. Chem. Soc.* **1999**, *121*, 7925.

(11) Snow, P. A.; Squire, E. K.; Russell, P. St. J.; Canham, L. T. *J. Appl. Phys.* **1999**, *86*, 1781.

(12) Yablonovitch, E.; Allara, D. L.; Tsang, C. C.; Gmitter, T.; Bright, T. B. *Phys. Rev. Lett.* **1986**, *57*, 249.

(13) Chazalviel, J.-N.; Ozanam, F. In *Structural and Optical Properties of Porous Silicon Nanostructures*; Amato, G., Delerue, C., von Bardeleben, C., Eds.; Gordon and Breach: Amsterdam, 1997; pp 53–71.

[†] Issued as NRCC Publication No. 43885.

^{*} To whom correspondence should be addressed.

[‡] Steacie Institute for Molecular Sciences.

[§] Institute for Chemical Process and Environmental Technology.

^{||} Institute for Microstructural Sciences.

[†] Current address: Petrie Science Building 351, Department of Chemistry, York University, 4700 Keele Street, Toronto, Ontario, Canada M3J 1P3.

(1) Canham, L. T. *Appl. Phys. Lett.* **1990**, *57*, 1046–1048.

(2) Cullis, A. G.; Canham, L. T.; Calcott, P. D. J. *J. Appl. Phys.* **1997**, *82*, 909–965.

(3) Motohashi, A.; Kawakami, M.; Aoyagi, H.; Kinoshita, A.; Satou, A. *Jpn. J. Appl. Phys., Part 1* **1995**, *34*, 5840.

to protect the PSi from PL fatigue.¹⁴ Deliberate oxidation of the surface is one of the most studied reactions to achieve this goal, under thermal, electrochemical, or chemical conditions.² Under controlled conditions, thermal oxidation provides good results in preserving a red surface-related PL^{15,16} and a light-emitting device based on thermally oxidized PSi was recently reported.¹⁷ However, passivation of the PSi surface by oxidation restricts the PL to red wavelengths and is not suitable for stabilizing the PL of high-porosity PSi. For example, blue photoluminescent PSi tends to react quickly with oxygen upon exposure to ambient air and the PL shifts after only a few seconds to the red.^{18,19} Recently, it has been found that etching of silicon single crystals in a mixture of hydrofluoric acid and ferric nitrate aqueous solution leads to a stable red photoluminescent PSi.²⁰ This effective passivation is attributed to the presence of Si-Fe bonds on the PSi surface. However, the presence of metals such as iron on the semiconductor surface may severely limit the use of PSi in advanced semiconductor technology.

More recently, there has been increasing interest in the chemical modification of silicon surfaces.²¹⁻⁴¹ This strategy has been used successfully in the passivation

of flat and porous silicon surfaces and in the preparation of organic monolayers chemically stable in different organic and aqueous media. Advantages associated with these transformations include the existence of a wide range of chemical functionalities compatible with the Si-H bonds terminating the PSi surface, the ease of carrying out the chemical reactions, and finally, the very well-established organosilicon chemistry in solution. Scaling down to the molecular level will open new opportunities for a new generation of devices.

Several methods have been shown to be useful for the preparation of organic monolayers covalently attached through Si-C and Si-O-C bonds to flat Si surfaces under photochemical,²²⁻²⁴ electrochemical,^{25,26} and thermal^{27,28} conditions as well as using a catalyst.²⁹ Recently, we reported that the direct reaction of Grignard reagents with the H-terminated surface Si(111)-H at 85 °C leads to the formation of organic monolayers that are stable in boiling aqueous and organic solvents.³⁰ We demonstrated that it is possible to control the organic functionalization on a Si(111) surface and carry out multistep reactions with high chemical yields.³¹ In addition, we have studied the thermal reaction of aldehydes and alcohols with Si(111)-H and have provided some insights into the mechanism by which these transformations take place.³²

Both the formation of Si-O-C and Si-C linkages on PSi have been studied. The formation of organic monolayers containing Si-OR linkages has been achieved by photoelectrochemical³³ reaction with carboxylic acids and electrochemical³⁴ and thermal³⁵ reaction with alcohols of freshly prepared PSi surfaces. Stabilization of the PSi surface through Si-C linkages was achieved by a direct reaction of hydrogen-terminated PSi surfaces with alkyl Grignards and lithium reagents under electrochemical³⁶ and thermal³⁷⁻³⁹ conditions. In the latter case, the reaction occurs with Si-Si bond cleavage to give Si-C and Si-M (M = Mg, Li) bonds. The latter intermediate could be functionalized with different electrophiles. Hydrosilylation of hydrogen-terminated surfaces with alkenes and alkynes was successfully applied in the presence of a Lewis acid as a catalyst⁴⁰ and by a thermal reaction at an elevated temperature⁴¹ to attach organic moieties through Si-C bonds.

In this report we investigate in more detail the noncatalytic thermally induced hydrosilylation of PSi surfaces with alkenes and aldehydes. While Bateman et al.⁴¹ first reported the thermal hydrosilylation of PSi-H by alkenes and alkynes, to our knowledge the work presented herein is the first report of the analogous reactions of aldehydes. We provide a more detailed characterization of surfaces functionalized by both reagents using DRIFT, transmission FTIR, Raman, and X-ray photoelectron spectroscopies. Chemical stability of these organic monolayers in different aqueous and organic media and auger electron spectroscopic (AES) depth profiling experiments are used to evaluate the uniformity of the chemical modification within the pores. These results are compared to analogous data recently reported by Buriak and co-workers⁴⁰ using a Lewis acid catalyst. We have examined the effect of these alkyl monolayers on the PL stability by aging in

- (14) Chazalviel, J.-N.; Ozanam, F. *MRS Conf. Proc.* **1999**, 536, 155.
 (15) Petrova-Koch, V.; Muschik, T.; Kux, A.; Meyer, B. K.; Koch, F.; Lehmann, V. *Appl. Phys. Lett.* **1992**, 61, 943.
 (16) Cullis, A. G.; Canham, L. T.; Williams, G. M.; Smith, P. W.; Dosser, Q. D. *J. Appl. Phys.* **1994**, 75, 493.
 (17) Hirschman, K. D.; Tsybeskov, L.; Duttagupta, S. P.; Fauchet, P. M. *Nature* **1996**, 384, 338.
 (18) Mizuno, H.; Koyama, H.; Koshida, N. *Appl. Phys. Lett.* **1996**, 69, 3779.
 (19) Wolkin, M. V.; Jorne, J.; Fauchet, P. M.; Allan, G.; Delerue, C. *Phys. Rev. Lett.* **1999**, 82, 197.
 (20) Zhang, Y. H.; Li, X. J.; Zheng, L.; Chen, Q. W. *Phys. Rev. Lett.* **1998**, 81, 1710.
 (21) Buriak, J. M. *Chem. Commun.* **1999**, 1051-1060.
 (22) Linford, M. R.; Chidsey, C. E. D. *J. Am. Chem. Soc.* **1993**, 115, 12631-12632.
 (23) Linford, M. R.; Fenter, P.; Eisenberger, P. M.; Chidsey, C. E. D. *J. Am. Chem. Soc.* **1995**, 117, 3145-3155.
 (24) Effenberger, F.; Gotz, G.; Bidlingmaier, B.; Wezstein, M. *Angew. Chem., Int. Ed.* **1998**, 37, 2462-2464.
 (25) de Villeneuve, C. H.; Pinson, J.; Bernard, M. C.; Allongue, P. *J. Phys. Chem. B* **1997**, 101, 2145.
 (26) Allongue, P.; de Villeneuve, C. H.; Pinson, J.; Ozanam, F.; Chazalviel, J. N.; Wallart, X. *Electrochim. Acta* **1998**, 43, 2791-2798.
 (27) Bansal, A.; Li, X.; Lauerman, I.; Lewis, N. S. *J. Am. Chem. Soc.* **1996**, 118, 7225-7226.
 (28) Sieval, A. B.; Semler, A. L.; Nissink, J. W. M.; Linford, M. R.; van der Maas, J. H.; de Jeu, W. H.; Zuillhof, H.; Sudholter, J. R. *Langmuir* **1998**, 14, 1759-1768.
 (29) Zazzera, L. A.; Evans, J. F.; Deruelle, M.; Tirrell, M.; Kessel, C. R.; McKeown, P. *J. Electrochem. Soc.* **1997**, 144, 2184.
 (30) Boukherroub, R.; Bensebaa, F.; Morin, S.; Wayner, D. D. M. *Langmuir* **1999**, 15, 3831-3835.
 (31) Boukherroub, R.; Wayner, D. D. M. *J. Am. Chem. Soc.* **1999**, 121, 11513-11515.
 (32) Boukherroub, R.; Morin, S.; Sharpe, P.; Wayner, D. D. M.; P. Allongue. *Langmuir* **2000**, 16, 7429-7434.
 (33) Lee, E. J.; Bitner, T. W.; Ha, J. S.; Shane, M. J.; Sailor, M. J. *J. Am. Chem. Soc.* **1996**, 118, 5375-5382.
 (34) Warntjes, M.; Vieillard, C.; Ozanam, F.; Chazalviel, J.-N. *J. Electrochem. Soc.* **1995**, 142, 4138-4142.
 (35) Kim, N. Y.; Laibinis, P. E. *J. Am. Chem. Soc.* **1997**, 119, 2297-2298.
 (36) Dubois, T.; Ozanam, F.; Chazalviel, J.-N. *ECS. Conf. Proc.* **1997**, 97-7, 296-310.
 (37) Song, J. H.; Sailor, M. J. *J. Am. Chem. Soc.* **1998**, 120, 2376-2381.
 (38) Kim, N. Y.; Laibinis, P. E. *J. Am. Chem. Soc.* **1999**, 121, 7162-7163.
 (39) Kim, N. Y.; Laibinis, P. E. *J. Am. Chem. Soc.* **1998**, 120, 4516-4517.
 (40) Buriak, J. M.; Allen, M. J. *J. Am. Chem. Soc.* **1998**, 120, 1339-1340. (b) Buriak, J. M.; Stewart, M. P.; Geders, T. W.; Allen, M. J.; Choi, H. C.; Smith, J.; Raftery, D.; Canham, L. T. *J. Am. Chem. Soc.* **1999**, 121, 11491-11502.

(41) Bateman, J. E.; Eagling, R. D.; Worall, D. R.; Horrocks, B. R.; Houlton, A. *Angew. Chem., Int. Ed.* **1998**, 37, 2683-2685.

ambient air and by a more aggressive treatment with steam for several months. Raman spectroscopy was found very useful in monitoring the change of the intrinsic properties of the porous layer during the aging process. The details of these studies, which result in ideal passivation of PSi, are reported in this paper.

Experimental Section

Silicon wafers were purchased from Virginia Semiconductor. All cleaning and etching reagents were clean room grade (Olin Microelectronics Materials). All other reagents were obtained from Aldrich and were the highest purity available.

Sample Preparation. Single side polished (100) oriented p-type silicon wafers (B-doped, 1–1.05 Ω -cm resistivity) were first cleaned in 3:1 concentrated H_2SO_4 /30% H_2O_2 for 5 min at room temperature and then rinsed copiously with Milli-Q water. The clean wafers were immersed in 48% aqueous HF solution for 1 min at room temperature to remove the native oxide. The hydrogen-terminated surfaces were electrochemically etched in a 1:1 (v/v) pure ethanol and 48% aqueous HF for 8 min at a current density of 5 mA/cm². After etching, the samples were rinsed with pure ethanol and dried under a stream of dry nitrogen prior to use. Atomic force microscopy (AFM) in contact mode showed that PSi films prepared in this way are 2.5–3- μm thick with an average pore diameter of ca. 7 nm.

PSi Functionalization. The freshly prepared PSi surface was placed under argon in a Schlenk tube containing a deoxygenated neat 1-decene or aldehyde and allowed to react at 115 or 85 $^\circ\text{C}$, respectively, for 16 h. The excess of unreacted and physisorbed reagent was removed by rinsing, at room temperature, with tetrahydrofuran and 1,1,1-trichloroethane and then the sample was dried under a stream of nitrogen.

Steam Treatment. Samples were aged by exposure to 100% humidity air at 70 $^\circ\text{C}$. A simple apparatus was constructed in which a stream of argon was passed through boiling Milli-Q water and carried to the sample in a Soxhlet extractor above the boiling water.⁴² The temperature in the extractor was measured to be 70 $^\circ\text{C}$.

Atomic Force Microscopy. Atomic force microscopy (AFM) was carried out using a Digital Instruments MultiMode AFM equipped with a Nanoscope IIIa controller. AFM images were acquired at 0.5 Hz in contact mode using silicon nitride sharpened tips (Digital Instruments, 0.12 N m⁻¹) at a constant force of 1–2 nN. All images are leveled but otherwise unfiltered. To characterize the PSi layer thickness, the sample was cleaved through its center to produce very sharp and clean edges. One-half of the PSi sample was mounted edgewise in epoxy for cross-sectional analysis while the other was used to characterize the top surface.

X-ray Analysis. The density of the PSi layer was determined by low-angle X-ray scattering.⁴³ The specular reflectivity from the sample was measured using a Philips MRD diffractometer equipped with a four-crystal monochromator (220 reflections) and a 0.1-mm receiving slit. The index of refraction of a solid surface at X-ray wavelengths is slightly less than unity and results in total reflection of X-rays up to a critical angle typically of a few tenths of a degree. In the reflectivity curve, the critical angle corresponds to the angle at which the reflectivity starts to decrease sharply because of increased penetration of X-rays through the solid. The critical angle is proportional to the square root of the electronic density and its measurement provides an easy and accurate means of determining the density of materials at a solid surface. In the low-angle reflectivity scan shown in Figure 1, three distinct steps are seen at angles of incidence of 0.074 $^\circ$, 0.12 $^\circ$, and 0.22 $^\circ$. The latter corresponds to the critical angle of the silicon substrate. The second step corresponds to an overlayer of density about 30% that of crystalline Si (i.e., a porosity of 70%).

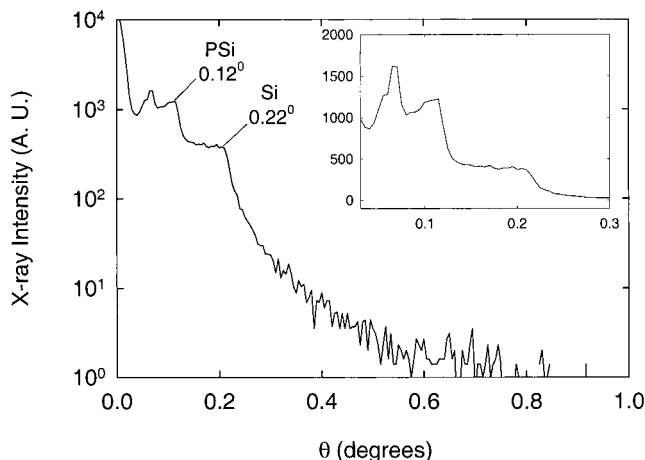


Figure 1. X-ray reflectivity response for freshly prepared and H-terminated PSi at room temperature.

The first plateau would correspond to a more porous layer of density about 10% that of crystalline Si. However, this lower angle peak was shown to be an instrumental artifact as it is seen in this position on samples of varying preparation conditions as well as with untreated silicon.

Raman Analysis and Steady-State Room-Temperature PL. Raman and PL measurements were performed at room temperature in a quasi-backscattering geometry⁴⁴ using 30 mW of Ar⁺ laser excitation at 457.9 nm. The sample was cooled with a stream of helium gas to avoid laser heating and subsequent damage of the material.

FTIR Analysis. Diffuse reflectance infrared Fourier transform (DRIFT) spectra were recorded using a Nicolet MAGNA-IR 860 spectrometer at 2-cm⁻¹ resolution. The samples were mounted in a purged sample chamber. Background spectra were obtained using a freshly hydrogenated surface.

XPS Analysis. X-ray photoelectron spectra (XPS) were recorded on a Kratos Axis Instrument, using monochromated Al K α (1486 eV) radiation with detection on the surface normal. The pressure during analysis was about 5×10^{-8} Torr.

Auger Electron Spectroscopy. Auger analysis was performed on a Physical Electronic Industries PHI 650 instrument with a 5-keV electron beam 30 $^\circ$ off normal. An argon ion gun operating at 1 keV and 51 $^\circ$ off normal was used for depth profiling. The Si LMM, C KLL, and O KLL Auger lines at 96, 272, and 510 eV, respectively, were used to obtain the PSi composition profile. A sputter rate of 100 nm/min was determined from a Dektak profilometer trace of the ion-beam crater wall.

Results and Discussion

Atomic Force Microscopy. Characteristic cross-sectional images of the PSi samples using contact mode AFM are shown in Figure 2. The PSi layer shown was obtained after 8 min of etching at a current density of 5 mA cm⁻² in HF/EtOH = 1:1 (v/v) at room temperature. Three regions are visible in Figure 2a. The Si substrate appears at the bottom of the image as the very smooth gray surface. The PSi layer is the roughened surface in the central part of the image. Beyond the PSi/air interface (black region at the top of the image) the tip begins to fall off the sample. The position of the PSi/air layer interface is seen clearly from a line scan passing through the three regions of the image (see Figure 2b). The gradual drop-off beyond the PSi/air interface is due to continued contact with the edge of the pyramidal tip. From this image the average thickness of the PSi layer is $2.6 \pm 0.06 \mu\text{m}$.

(42) Neuwald, U.; Hessel, H. E.; Feltz, A.; Memmert, U.; Behm, H. *J. Appl. Phys. Lett.* **1992**, *60*, 1307–1309.

(43) Buttard, D.; Dolino, G.; Bellet, D.; Baumbach, T.; Rieutord, F. *Solid State Commun.* **1999**, *109*, 1–5.

(44) Lockwood, D. J.; Dharma-Wardana, M. W. C.; Baribeau, J.-M.; Houghton, D. C. *Phys. Rev. B* **1987**, *35*, 2243–2251.

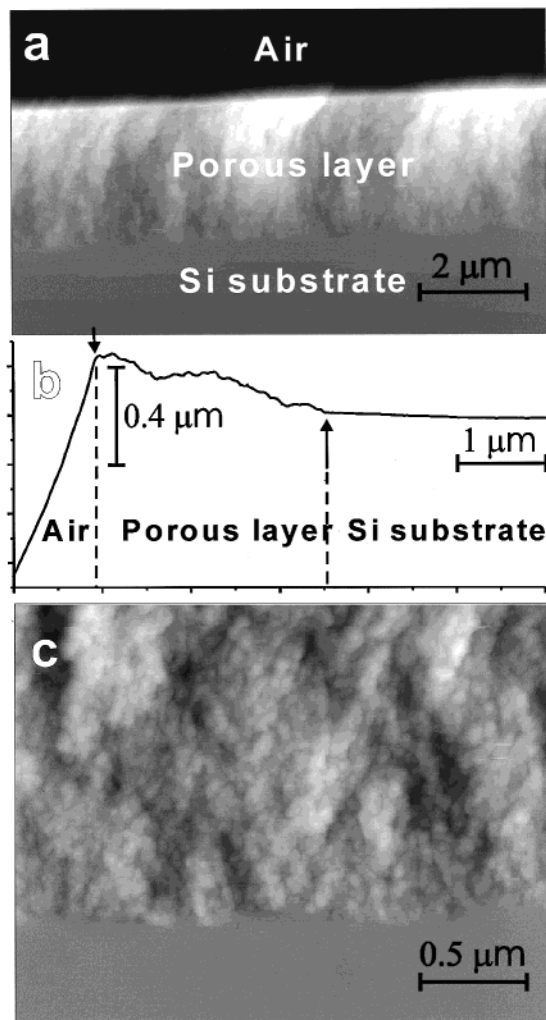


Figure 2. Contact mode AFM image of the cross section of a PSi layer (a) $10 \times 6 \mu\text{m}^2$; (b) line scan obtained from the central part of (a) for the height as a function of the length of the image (i.e., $6 \mu\text{m}$)—the three regions are indicated as well as the position of the interfaces (see arrows); and (c) detail of the porous layer/Si substrate interface, $2.5 \times 2.0 \mu\text{m}^2$.

By scanning over a smaller area that encompasses the porous layer/Si substrate interface, the granular structure of the PSi layer is evident (Figure 2c). On this scale, these structures ($50 \pm 20 \text{ nm}$ diameter) appear to be evenly distributed. When the tip is very close to the edge (not shown), it is more difficult to image the sample without interference from the PSi/air interface and it is thus more difficult to comment on the homogeneity of the crystallite size distribution in that region. Hence, one cannot rule out the possibility of a small porosity gradient near this interface. The PSi layer is clearly mesoporous, as often observed for Si etched in dilute aqueous HF or ethanolic HF (pore size smaller than 50 nm).²

Characterization of the Derivatized PSi Surfaces. Hydrosilylation of hydrogen-terminated PSi surfaces with 1-decene and with octanal and decanal takes place respectively at 115 and 85°C to give organic monolayers covalently attached to the surface through Si–C and Si–O–C bonds (Scheme 1).

A DRIFT or transmission FTIR spectrum of freshly prepared PSi (Figure 3a) is similar to that reported by Buriak.^{40b} The spectrum exhibits absorptions for the Si–H_x stretches modes (2088 cm^{-1} for $\nu_{\text{Si-H}_1}$, 2117 cm^{-1} for

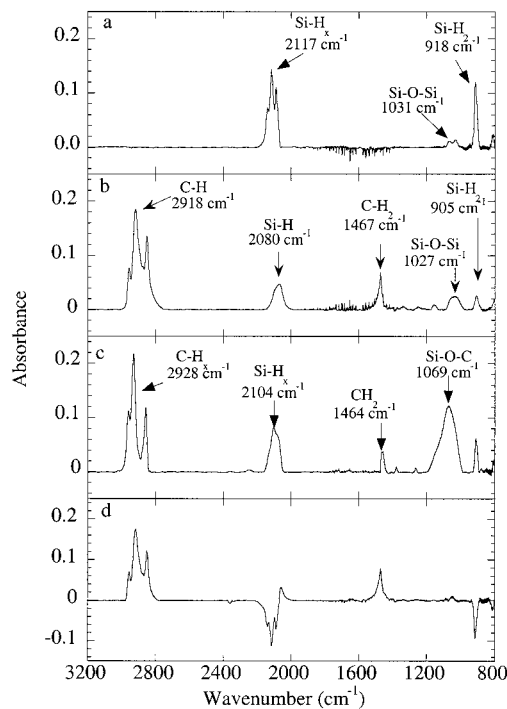
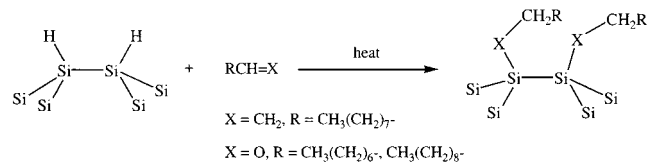


Figure 3. Diffuse reflectance infrared Fourier transform spectra for (a) freshly prepared PSi before functionalization and PSi derivatized with (b) 1-decene and (c) decylaldehyde, and a (d) difference DRIFTS spectrum of (b)–(a).

Scheme 1



$\nu_{\text{Si-H}_2}$, and 2138 cm^{-1} for $\nu_{\text{Si-H}_3}$), the Si–H₂ scissor mode (918 cm^{-1}) and the Si–O–Si stretch (due to interstitial oxygen in the original silicon substrate lattice, 1031 cm^{-1}). After the reaction of the PSi with 1-decene at 115°C (Figure 3b) or decanal at 85°C (Figure 3c) for 16 h, additional peaks at $2857\text{--}2960 \text{ cm}^{-1}$ (C–H stretching modes of the alkyl chain) and at 1470 cm^{-1} (methylene bending modes) appear.

The absorption intensity of $\nu_{\text{Si-H}_x}$ and $\delta_{\text{Si-H}_2}$ decreases substantially after the reaction, indicating that most of the hydrogen has reacted with the unsaturated C=C and C=O double bonds (Figure 3d). This result is consistent with a hydrosilylation reaction that preferentially consumes the more reactive SiH₃ and SiH₂ species (negative bands for the SiH_x stretch modes around 2117 cm^{-1} and the Si–H₂ scissors mode at 915 cm^{-1}). The DRIFT spectrum also indicates the presence of unreacted silicon–hydrogen bonds SiH₁ (2063 cm^{-1}) after the thermal modification of the PSi surfaces. Reaction for longer times does not increase the coverage, which appears to be limited by the steric hindrance introduced by the organic molecules on the surface.

The efficiency of the reaction as determined by the fraction of SiH_x stretch that disappears is 30–50% depending on the method of preparation of the PSi. We were perplexed to find that lower apparent conversions were obtained when the vibrational spectroscopic analysis was carried out using transmission FTIR on samples etched at low current densities (5 mA/cm^2 , $3\text{-}\mu\text{m}$ thick)

compared to DRIFT. However, for samples etched at higher current densities ($>100 \text{ mA/cm}^2$, $3\text{-}\mu\text{m}$ thick) there is good agreement between the two methods. Furthermore, there is good agreement between the two methods for samples etched at 5 mA/cm^2 to a thickness of $1 \mu\text{m}$. The reasons for the discrepancy in the low current density samples is not completely understood. In general, there are two factors that complicate the DRIFT analyses. The first is that the film thickness used in this study (ca. $3 \mu\text{m}$) leads to interference fringes that are about 100 times the peak width, leading to significant errors in baseline correction for absorption peaks on the rising or falling edges. The second is that the chemical modification significantly alters the optical properties of the film so the as-anodized film cannot be used to subtract out the interference fringes. The much higher frequency interference fringes in transmission measurements are easily filtered out of the spectrum. For the entire range of samples studied, transmission FTIR gives the most consistent and reliable data.

In all cases we found that the modification took place without measurable oxidation of the surface as indicated by the peak at 1031 cm^{-1} , which does not increase (in contrast to that reported by Bateman et al.⁴¹). The modification of the surface is accompanied by a decrease of the intensity and a broadening of the Si-H_x band. The broadening effect is likely related to the interactions of the unreacted Si-H_x with the organic molecules attached to the surface. Such a broadening effect has been reported for organic physisorbed molecules on hydrogen-terminated Si (111).^{45,46} A similar infrared spectrum was obtained when the as-anodized PSi sample was allowed to react with decyl aldehyde at $85 \text{ }^\circ\text{C}$ for 16 h, with an additional peak appearing at 1069 cm^{-1} that is consistent with the formation of Si-O-C bonds (Figure 3c).

X-ray photoelectron spectroscopy (XPS) was used to analyze the elemental composition of the PSi surfaces and the nature of the chemical bonding of the organic molecules on the surface. An XP survey spectrum of the as-anodized PSi contains small peaks at a binding energy of 687 and 532 eV due to the remaining fluoride ions in the silicon pores and the interstitial oxygen in the silicon lattice and an intense signal at 99 eV due to silicon (Figure 4a).

Figure 4b exhibits an XPS survey of the modified surface with 1-decene. The oxygen signal at 532 eV does not increase significantly. However, as expected, a new peak at 285 eV arising from C 1s of the alkyl chain appears. High-resolution XP spectra of Si 2p and C 1s (Figure 5a and b) of the decyl-terminated surface are consistent with the formation of an Si-C bond. The Si 2p is comparable to that from a hydrogen-terminated surface (Figure 5d). The small oxygen peak in the survey spectrum is not associated with surface oxidation (SiO₂), which would appear as a chemically shifted peak near 103 eV at high resolution.

The Si and C peaks in the XP spectrum of the decanal-modified PSi are similar to the decene-modified surface. In addition, the expected increase of the oxygen signal due to the Si-O-C link is observed. (Figure 4c). High-

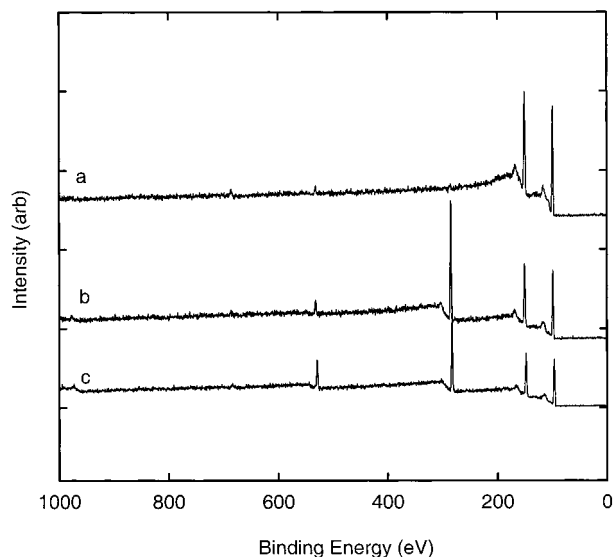


Figure 4. XPS survey of freshly prepared PSi substrate (a) and thermally modified PSi samples with (b) 1-decene and (c) decanal.

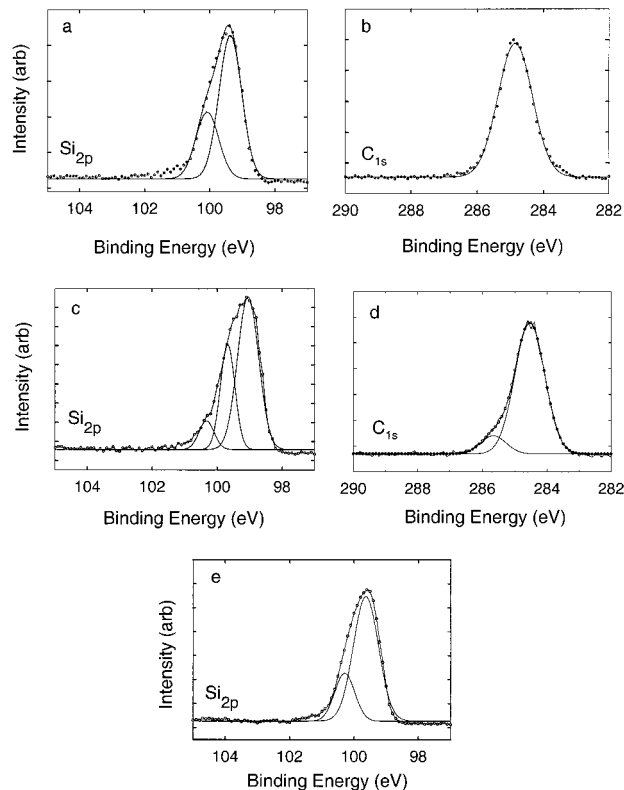


Figure 5. High-resolution XPS spectra of the Si 2p (left) and C 1s (right) regions of PSi surfaces prepared by the thermal reaction of H-terminated PSi with 1-decene (a), and decyl aldehyde (b). Si 2p of the as-anodized PSi is shown in (e).

resolution XP spectra are characterized by chemically shifted C 1s and Si 2p peaks, assigned to the respective carbon-oxygen (C-O) and silicon-oxygen (Si-O-C) linkages (Figure 5c and d). As with the decene-modified surface, there is no apparent peak due to silicon oxide. This supports our conclusion that these surface transformations occur without any conventional oxidation of the silicon surface.

Vibrational Raman spectroscopy was used to characterize the chemical state of the various PSi samples.

(45) Ye, S.; Ichihara, T.; Uosaki, K. *Appl. Phys. Lett.* **1999**, *75*, 1562-1564.

(46) Lopinski, G. L.; DeJong, K.; Wolkow, R. A., to be submitted.

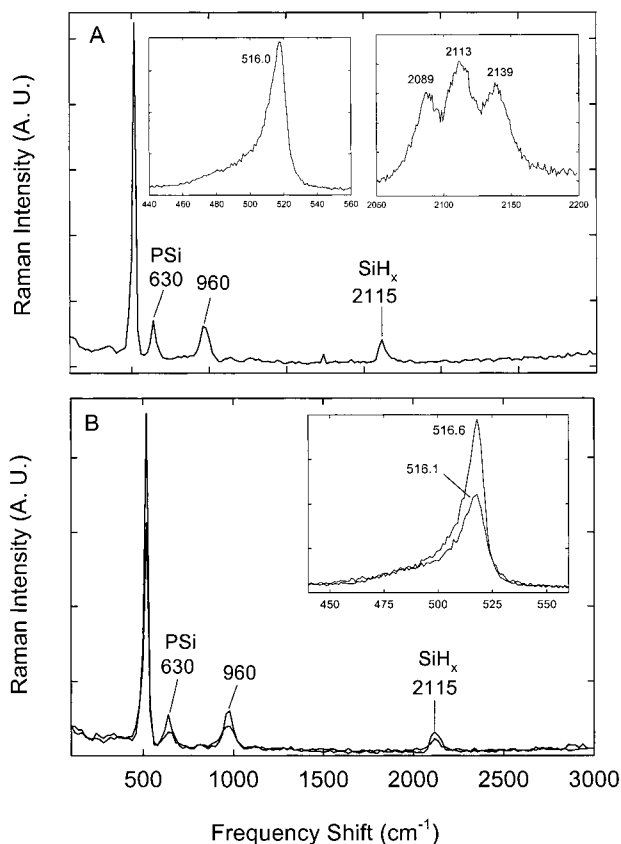


Figure 6. (A) Raman spectrum of freshly prepared H-passivated PSi recorded at room temperature with a resolution of 8 cm^{-1} and a step size of 20 cm^{-1} and (B) Raman spectra of freshly prepared PSi at room temperature before and after passivation with 1-decene. The insets show details of the spectrum recorded with a resolution of 3 cm^{-1} and step size of 1 cm^{-1} .

Like infrared spectroscopy, Raman scattering is sensitive to chemical bond formation, but has the additional advantage in this case of providing such information simultaneously with the PL measurements at the same location on the sample. The Raman spectrum of a freshly prepared sample of PSi is shown in Figure 6A. The intense peak at 516 cm^{-1} , shown in detail in the inset, is due to the nanostructured PSi layer. The Raman frequency of crystalline silicon (c-Si) is 520 cm^{-1} , but this peak is not evident in Figure 6A. This indicates that the blue excitation light at 457.9 nm does not penetrate through the $2\text{-}\mu\text{m}$ -thick PSi layer to reach the c-Si substrate. The weaker features (e.g., 630 and 960 cm^{-1}) at frequencies less than 1000 cm^{-1} are due to second-order scattering from PSi. The peak at $\sim 2115\text{ cm}^{-1}$ actually comprises three bands at 2089 , 2113 , and 2139 cm^{-1} (see inset): these correspond to various Si-H_x stretching vibrations also seen in the infrared at 2088 , 2117 , and 2138 cm^{-1} . No other Raman features were observed in any of the freshly prepared PSi samples.

The Raman frequency of $516 \pm 0.4\text{ cm}^{-1}$ found for the porous silicon samples allows a determination of the average nanoparticle diameter.^{47,48} From the known dependence of the silicon Raman frequency on silicon

sphere diameter,⁴⁹ the frequency shift from 520 cm^{-1} in c-Si to 516 cm^{-1} in PSi indicates an average spherulite diameter of 5 nm .

The Raman spectrum of a freshly prepared PSi sample before and after reacting with 1-decene is shown in Figure 6B. The spectra are identical in feature position and line shape, with the exception of a weak broad band appearing at 2900 cm^{-1} due to the alkyl C-H vibrations. The latter sample exhibits a 30% lower Raman intensity characteristic of the coated PSi layer. The inset to Figure 6B confirms that the PSi structure is unaffected by passivation. Similar results were obtained from Raman measurements of the modified surfaces with octyl and decyl aldehydes. The Raman spectra also show, in agreement with the DRIFTS results, that not all of the passivating H atoms are removed in the thermal activation process.

Even though the majority of the Si-H bonds terminating the PSi surface was consumed, as evidenced by IR and Raman results, it was still unclear at this point if the hydrosilylation reaction occurred only at the external surface, leaving the internal surface of the pores intact. If this were the case, this method would be ineffective for long-term electronic passivation of the porous layers. To characterize the elemental composition of the internal surfaces of the modified PSi substrates, we used Auger profiling and scanned directly through the porous layer.

Figure 7 displays Auger depth profiles of the PSi and a modified PSi surface. The as-anodized surface (Figure 7a) shows a constant atomic concentration of silicon with carbon and oxygen both below the detection limit. As a control, the as-anodized surface was heated in deoxygenated decane at $100\text{ }^\circ\text{C}$ for 22 h (Figure 7b). After this treatment there was a barely perceptible increase in the methylene absorption in the vibrational spectrum of the film but no measurable decrease in the Si-H absorption. The Auger depth profile of this surface shows only traces of physisorbed carbon with the oxygen still below the detection limit. After modification with decene (Figure 7c) there is a clear increase in the carbon content, which is constant from the surface to the PSi/Si interface, thus showing that the pores are uniformly modified. Similar results are obtained for the aldehyde-modified surface (data not shown) with the difference that there is a constant concentration of both carbon and oxygen throughout the porous region with relative concentrations consistent with elemental composition of the monolayer. The increase of the Si concentration and the abrupt disappearance of the carbon signal provides a clear measure of the PSi/Si interface. These results, which are qualitatively similar to SIMS depth profiling reported by Buriak and co-workers^{40b} for the catalytic process, argue for the chemical attachment of organic molecules throughout the internal surfaces of the PSi and further confirm that this method is very efficient for the passivation of the internal surface.

Stability of the Monolayers. Long-term passivation of the PSi requires a protecting organic layer, which does not produce surface states and is chemically robust. To evaluate the chemical robustness of the surface derivatized with 1-decene, samples were subjected to

(47) Richter, H.; Wang, Z. P.; Ley, L. *Solid State Commun.* **1981**, *39*, 625–629.

(48) Lockwood, D. J. *Solid State Commun.* **1994**, *92*, 101–112.

(49) Campbell, I. H.; Fauchet, P. M. *Solid State Commun.* **1986**, *58*, 739–741.

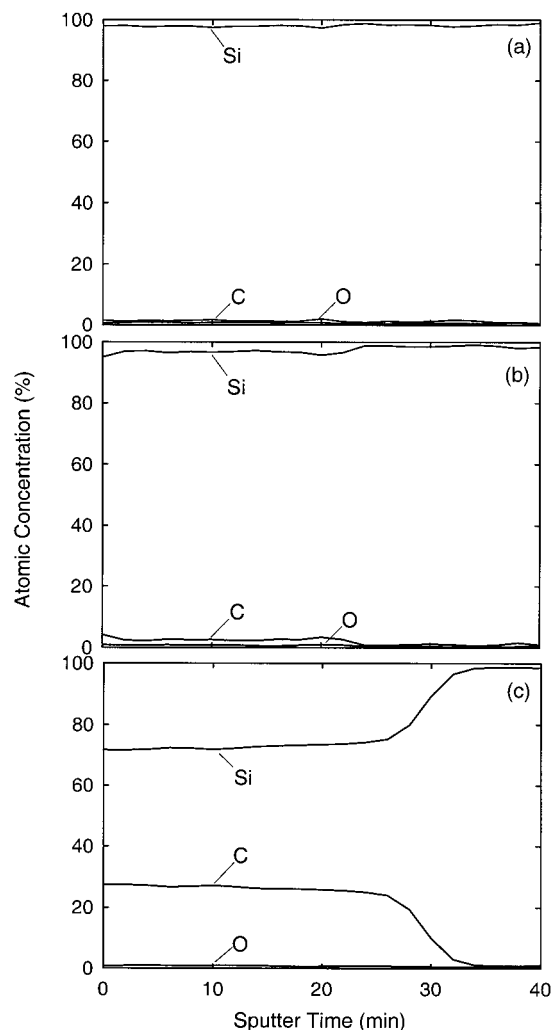


Figure 7. Auger profiles of (a) as-anodized PSi, (b) as-anodized PSi heated in deoxygenated decane for 22 h at 100 °C, and (c) PSi modified with decene.

the following sequential treatments: sonication in CH_2Cl_2 for 5 min at room temperature, boiling in CHCl_3 for 1 h, boiling in water for 1 h, immersion in Milli-Q water for 16 h at room temperature, immersion in 1.2 N HCl at 75 °C for 2 h, and immersion in aqueous 48% HF solution for 65 h at room temperature. The decene-modified surface was found to be extremely robust; there was no evidence for any chemical deterioration of the monolayer as evidenced by the unchanged $\nu_{(\text{C-H})}$ IR intensity associated with the alkyl group (Figure 8). After these chemical treatments there was no evidence of oxidation of the silicon surface (i.e., no increase of the $\nu(\text{Si-O})$ absorbance). The hydrophobic character of the methyl end groups of the alkyl chain and the high coverage of the surface prevents the permeation and diffusion of aqueous and organic molecules and thus ideally chemically passivate the surface. The chemical stability is not affected, even in harsh environments such as aqueous HF solutions at room temperature or KOH solutions (pH 13) for several hours. The aldehyde-modified surfaces also are stable under the same conditions.

Reaction Mechanism. The IR results clearly show that the thermal reaction of 1-alkenes and aldehydes occurs with the consumption of Si-H bonds. This is consistent with the addition of the weak Si-H bond

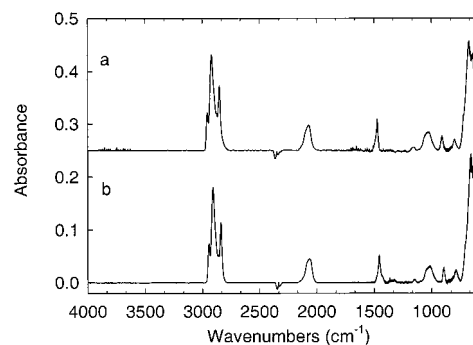
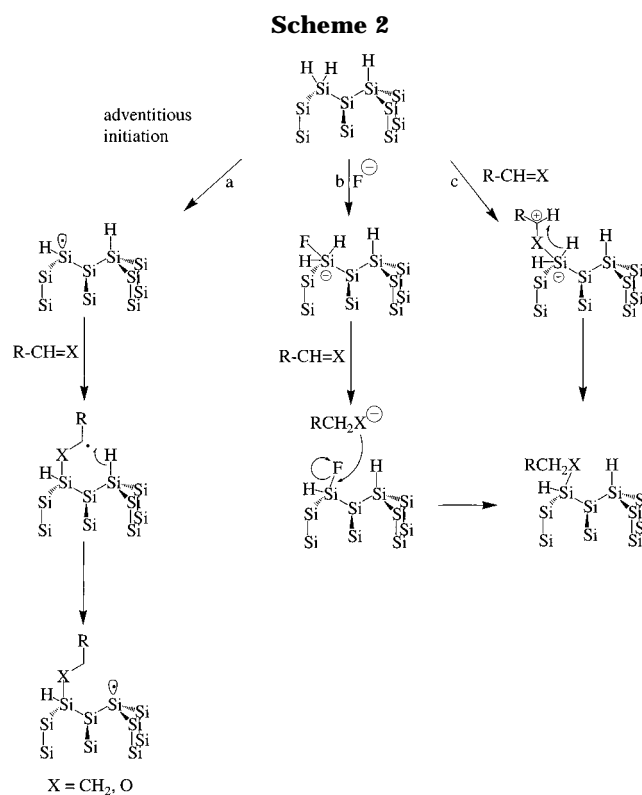


Figure 8. DRIFT spectra of (a) freshly prepared decyl-terminated PSi surface and (b) the derivatized surface after the following sequential treatments: sonication in CH_2Cl_2 for 5 min, at room temperature, boiling in CHCl_3 for 1 h, boiling in water for 1 h, immersion in Milli-Q water for 16 h at room temperature, immersion in 1.2 N HCl at 75 °C for 2 h, immersion in aqueous 48% HF solution for 2 h at room temperature, and immersion in 48% HF for 65 h at room temperature.



across the unsaturated double bond ($\text{C}=\text{X}$, $\text{X}=\text{O}$, CH_2) and not with the cleavage of the Si-Si bonds, as reported for the thermal reaction of PSi with alcohols,³⁵ alkyllithium,^{37,38} and Grignard³⁹ reagents. On the basis of these observations, three possible reaction pathways for this hydrosilylation reaction are envisioned. The first mechanism is a surface radical chain reaction that would be initiated by adventitious radical formation (Scheme 2a) and is similar to the mechanism reported by Chidsey et al.²³ for alkene addition to Si(111)-H single-crystal surfaces. The second mechanism is a fluoride-catalyzed stepwise mechanism in which the first step corresponds to the nucleophilic attack of fluoride ions remaining on the surface or in the pores on the silicon center to form a pentavalent Si intermediate $\text{Si}(\text{H})(\text{F})$, which could then transfer a hydride to the double bond to give an anion (RCH_2-X^- , $\text{X}=\text{O}$, CH_2)

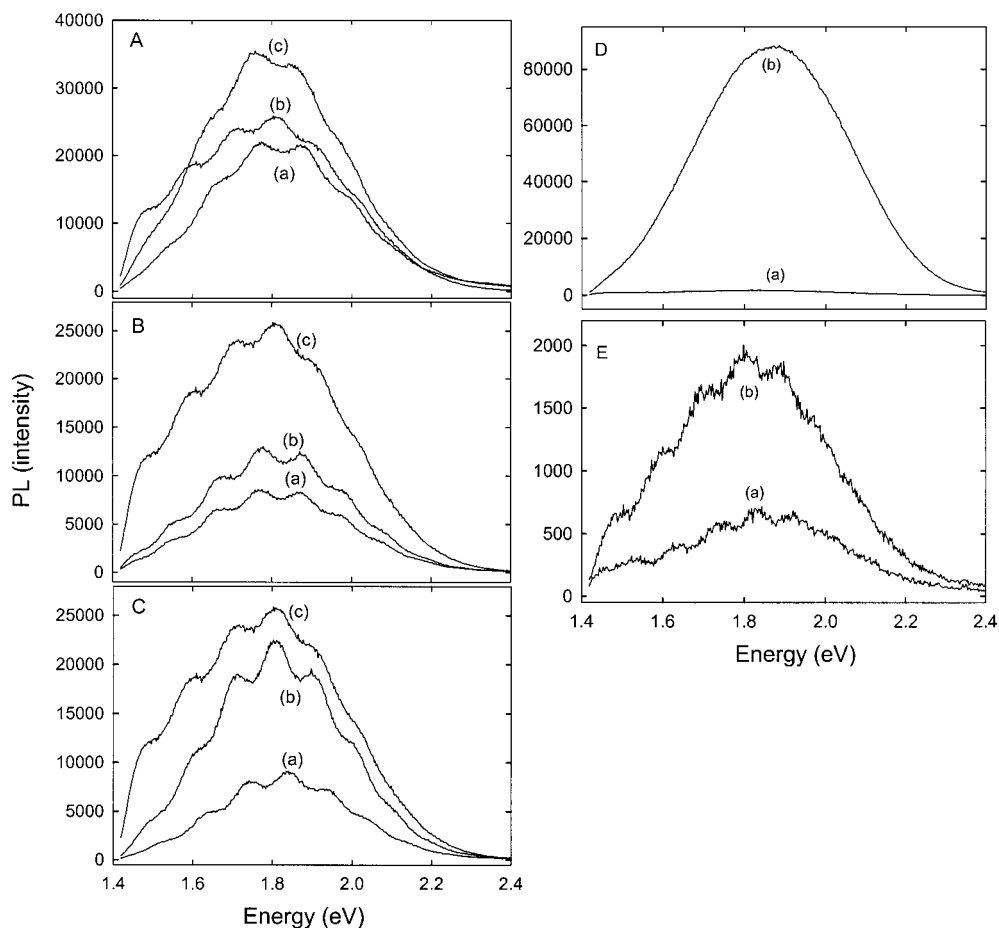


Figure 9. Steady-state room temperature PL spectra of A: derivatized PSi with octyl aldehyde (a), freshly prepared PSi (b), and (a) steam treated for 3 days (c). B: freshly prepared decyl aldehyde modified PSi surface (a), as-anodized PSi (b), and (a) steam treated for 3 days (c). C: freshly prepared 1-decene modified PSi surface (a), as-anodized PSi (b), and (a) steam treated 3 days (c). D: as-anodized PSi before (a) and after 6 weeks steam treatment (b). E: freshly prepared 1-decene functionalized surface before (a) and after 6 weeks of steam treatment (b).

and a subsequent nucleophilic attack of the anion on Si will lead to the product formation (Scheme 2b). The third mechanism is very similar to the second, except that the π -electron rich double bond attacks the silicon center to form a pentavalent silicon intermediate or transition state followed by a [1,3]-hydride shift (Scheme 2c).

A few points remain unclear concerning the first mechanism. On one hand, it is unlikely that there are any remaining dangling bonds on the surface that could initiate the radical chain. These species are too reactive to survive the rinsing and the transfer steps. On the other hand, the rate constants for addition of silicon-centered radicals to carbonyls is about the same as those for alkenes; the reaction of aldehydes occurs at 85 °C or lower while the direct addition of the alkenes takes place at higher temperature (115 °C). The same behavior was observed on the crystalline silicon Si.^{28,22} Another argument against the radical chemistry arises from the recent observation by Buriak et al.⁵⁰ concerning the white light-promoted hydrosilylation of PSi surfaces with alkenes and alkynes. They found that electron-deficient alkynes require longer reaction times. (It is known that electron-deficient alkynes react more rapidly with silicon-centered radicals).

Even though the ease of expanding coordination at silicon, in solution, is very well documented in the literature,⁵¹ there are no examples reported for analogous processes in the surface chemistry literature. We raise the possibility because there is some residual fluoride remaining in the pores after the etching process and because this strategy was successfully used in molecular organosilicon chemistry for aldehyde reduction with organosilicon hydrides assisted by fluoride ions.^{52,53} In the case of the fluoride ion, the reaction is favorable from the steric, thermodynamic, and kinetic perspectives. While the polar character of the C=O bond in the case of aldehydes facilitates the hydride transfer to yield the corresponding alkoxide, there is no precedent in the literature for the hydride addition to the carbon-carbon double bond to yield the corresponding carbanion (RCH_2^-). At this stage, we prefer the last of the three mechanisms, although without more experimental data, the other pathways cannot be unequivocally ruled out.

Steady-State Photoluminescence (PL). Typical PL spectra of freshly prepared PSi before and after modification with octanal are shown in Figure 9A. The

(51) Corriu, R. J. R.; Guerin, C.; Moreau, J. J. E. *Top. Stereochem.* **1984**, *15*, 43.

(52) Fry, J. L.; McAdam, M. A. *Tetrahedron Lett.* **1984**, *25*, 5859–5862.

(53) Fujita, M.; Hiyama, T. *J. Org. Chem.* **1988**, *53*, 5405–5415.

(50) Stewart, M. P.; Buriak, J. M. *Angew. Chem., Int. Ed.* **1998**, *37*, 3257–3260.

PL intensity and the peak position were not affected by the derivatization. The functionalized sample exhibits an orange-red photoluminescence comparable to the H-terminated sample Figure 9A(b), which is characteristic of 70% porosity. Aging the samples in air for several months, in the dark or exposed to daylight, does not induce any change in the PL intensity or in the energy maximum. When the organic-passivated substrate was exposed to 100% humidity air at 70 °C for 3 days (Figure 9A(c)), there was an increase in intensity by about 40%. Samples modified with decanal, Figure 9B(a), showed a reduction of the PL of about 60% compared to a freshly etched sample (Figure 9B(c)). Aging in ambient air does not have any effect on the PL intensity, even after 2 months. Steam treatment for 3 days results in an increase in the PL intensity of 35% (Figure 9B(b)). Further exposure to steam has little effect on the PL intensity.

The PL spectrum of the decyl-terminated surface is shown in Figure 9C. The PL intensity is only 40% of the as-anodized PSi sample (Figure 9C(c)). Aging for 3 days under the same conditions as for the octanal- and decanal-modified surfaces results in an increase in the PL intensity of only 50% (Figure 9C(b)). Again, exposure to 100% humidity air at 70 °C for 6 weeks had a relatively small effect on the PL nor on the PL maximum. The PL intensity of the modified sample increased by about a factor of 3, Figure 9D(b), compared to the original PL, measured just after chemical modification. However, the PL of the as-anodized sample had increased by a factor of 50 under the same conditions (Figure 9E). Maruyama et al.⁵⁴ reported a similar aging effect on the PL intensity of as-anodized PSi in ambient air. They observed that the PL intensity increased dramatically and exhibited a red shift when exposed to humid air at room temperature. They assigned this change to a gradual oxidation of the PSi skeleton, based on structural studies (IR and XPS spectroscopies).

The reduction of the PL from the thermal reaction of decene is less than that from the catalytically modified surface in which the PL efficiency was only 25% of the hydrogen-terminated sample.^{40b} Treatment with HF resulted in partial recovery to about 50% of the original intensity (coincidentally the level achieved initially in the thermal reaction). Treatment with HF had no effect on the PL intensity of the modified PSi in this study. Again, and consistent with the spectroscopic evidence, this suggests that the thermal reaction provides a more effective passivating layer, which renders the silicon inaccessible by polar solvents.

Raman, DRIFT, and transmission FTIR spectroscopies have been used as tools to monitor the intrinsic properties of the porous layer and to understand the aging effect on the PL intensity. For the functionalized surfaces, the Raman peak remains unchanged and shows the same features compared to the initially modified surfaces (before aging). The increase in the PL intensity is ascribed to the formation of a very small amount of oxide during the aging process (a small increase in the Si–O–Si stretching mode in the DRIFT spectrum) without any apparent loss of the organic layer. Similar results were reported by Chazalviel et al.

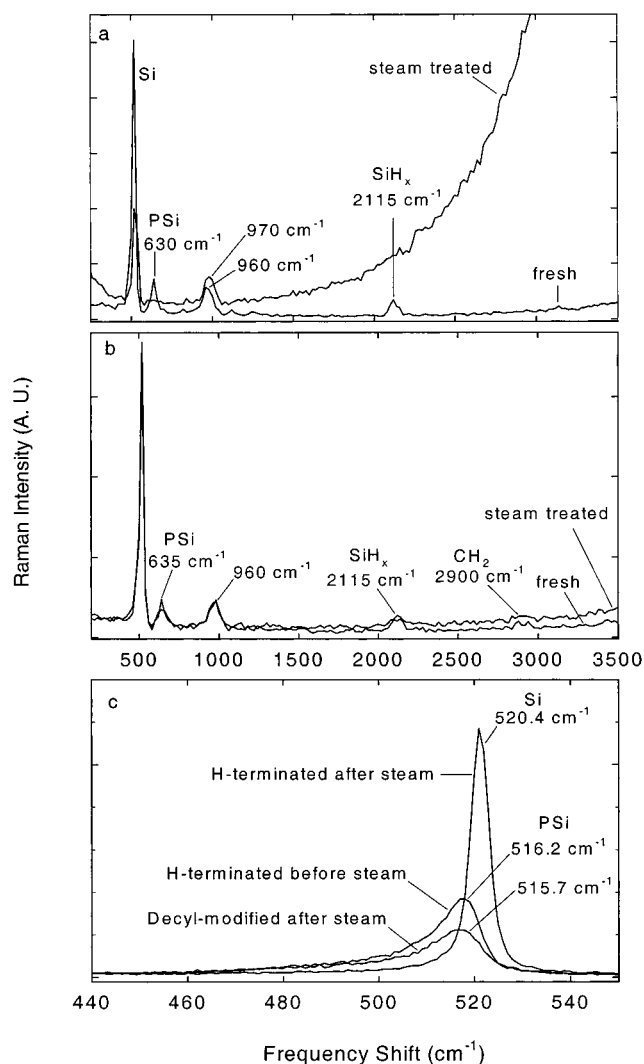


Figure 10. Raman spectra of (a) H-terminated PSi and (b) decyl-modified PSi before and after steam treatment for 6 weeks, and (c) gives details of the Si peak before and after steam treatment for 6 weeks. See the caption of Figure 6 for other experimental details.

for electrochemically methylated²² and methoxylated²⁰ PSi surfaces with a slight blue shift in the maximum intensity. The methoxylated surface lost the PL after aging in air for several days. Buriak et al.⁵⁵ have studied the aging effect on the PL fatigue of a PSi surfaces modified with 1-dodecene (prepared by a hydrosilylation reaction catalyzed by EtAlCl₂), soaked in HF/EtOH (30 min at room temperature), and boiled in aerated KOH/EtOH solutions (pH = 10, 2 h). They found that the PLs of both samples irradiated with a mercury lamp in air decay faster than freshly prepared H-terminated PSi.

Raman spectroscopy is particularly informative in understanding the effect of the aggressive steam oxidation on H-terminated porous silicon. The spectra given in Figure 10a shows that the first- and second-order silicon Raman features are considerably modified after steam treatment: the 630-cm⁻¹ line disappears and the 516- and 960-cm⁻¹ lines shift up to 520 and 970 cm⁻¹. Also, the SiH_x line at 2115 cm⁻¹ is no longer visible. The Si line at 520 cm⁻¹ is now sharp and symmetric, Figure 10b, and is typical of crystalline Si. The Raman

(54) Maruyama, T.; Ohtani, S. *Appl. Phys. Lett.* **1995**, *65*, 1346–1348.

(55) Buriak, J. M.; Allen, M. J. *J. Lumin.* **1999**, *80*, 29–35.

spectrum of the steam-treated sample indicates that the PSi layer has been converted to SiO_x , which is transparent to the blue incident light. On the other hand, the Raman spectrum of the decyl-terminated sample is unchanged by the same steam treatment, as can be seen in Figure 10c. The samples modified with octyl and decyl aldehydes behaved similarly.

DRIFT and transmission FTIR spectroscopies show that the hydrogen peak present in the H-terminated surface centered at 2117 cm^{-1} was shifted to 2249 cm^{-1} , characteristic of $[(-\text{O}-)_3\text{Si}-\text{H}]$, accompanied with an intense band at 1114 cm^{-1} corresponding to the stretching mode vibration of Si-O-Si. The drastic increase in the number of Si-O-Si bonds is attributed to the formation of a transparent oxide monolayer.

These results clearly demonstrate the unprecedented and extreme stability of the modified surfaces to harsh environmental conditions and the blocking and protective effect of the organic molecules against oxidation compared to hydrogen-terminated PSi.

Conclusions

We have shown that PSi substrates can be effectively passivated by organic functionalization of the hydrogen-terminated surfaces in a thermal, noncatalytic reaction. This transformation occurs with a high chemical yield and importantly retains the intrinsic structural proper-

ties of the PSi layers. Visible photoluminescence of the as-anodized PSi was preserved and found to be very stable during an aging process that completely destroyed underivatized surfaces. This includes exposure to 100% humidity at $70\text{ }^\circ\text{C}$ for as much as 6 weeks. The thermal reactions provide surfaces that are more densely packed (by about a factor of 2) than the corresponding surfaces modified in a catalytic process using Lewis acids. The difference between these processes is likely related to steric inhibition of the catalytic process, which requires the catalyst and the reactant to be in close proximity to the surface. Thus, the thermally modified surfaces have fewer defects. A similar decrease in coverage was reported for the catalytic modification of Si(111)-H surfaces.³⁰ The unprecedented high stability of the monolayers under such harsh conditions is an important step toward the development of PSi for potential photonic and sensor applications. It is expected that these modified surfaces will effectively prevent the hydrolytic corrosion of PSi layers in aqueous solutions and in simulated biological media.

Acknowledgment. The authors gratefully acknowledge Dr. Raluca Voicu for help with some of the DRIFT and transmission FTIR measurements.

CM000790B